New synthetic 1H-1,2,3-triazole derivatives of 3-O-acetyl-β-boswellic acid and 3-O-acetyl-11-keto-β-boswellic acid from *Boswellia sacra* inhibits carbonic anhydrase II *in vitro*

Satya Kumar Avula
University of Nizwa
Najeeb Rehman
University of Nizwa https://orcid.org/0000-0002-1563-225X
Majid Khan
University of Karachi
Sobia Ahsan Halim
University of Nizwa
Ajmal Khan
University of Nizwa
Kashif Rafiq
Mardan University: Abdul Wali Khan University Mardan
Rene Csuk
Martin-Luther-Universitat Halle-Wittenberg
Biswanath Das
University of Nizwa
Ahmed Al-Harrasi (aharrasi@unizwa.edu.om)
University of Nizwa

Research Article

Keywords: 3-O-acetyl-β-boswellic acid, 3-O-acetyl-11-keto-β-boswellic acid, 1H-1,2,3-triazole analogues, carbonic anhydrase II, inhibitor, molecular docking

Posted Date: February 19th, 2021

DOI: https://doi.org/10.21203/rs.3.rs-122986/v2

Version of Record: A version of this preprint was published at Medicinal Chemistry Research on March 31st, 2021. See the published version at https://doi.org/10.1007/s00044-021-02723-8.

Abstract

Boswellic acids are genus specific to *Boswellia*; they are the principal biologically active compounds holding exceptionally potent anti-inflammatory activity. A series of new 1*H*-1,2,3-triazole tethered of 3-*O*-acetyl-β-boswellic acid (ABA, **1**) and 3-*O*-acetyl-11-keto-β-boswellic acid (AKBA, **2**) derivatives (**10a-d** and **11a-d**) were synthesized and their carbonic anhydrase II (CA II) inhibitory activity was evaluated *in vitro*. All compounds were characterized by ^{1}H NMR, ^{13}C NMR, 2D NMR (HMBC, HSQC, COSY and NOESY) experiments, ESI-MS, and when applicable by ^{19}F NMR spectroscopy (**10b, 10c** and **11b, 11c**). This series has displayed a moderate to strong inhibition against CA II with IC_{50} values of 13.2–60.1 μM. All the active compounds were reported for the first time for their CA II inhibition potential. Kinetics studies on the most active inhibitors (**5** and **10b**) were carried out to investigate their mode of inhibition and to determine their inhibition constants K_i. Both compounds (**5** and **10b**) were found to be non-competitive inhibitors with K_i values of 10.40 ± 0.013 and 14.25 ± 0.017 μM, respectively. Molecular docking studies showed that all compounds were well accommodated in the allosteric site of CA II. The current study has demonstrated the usefulness of incorporating a 1*H*-1,2,3-triazole moiety into the boswellic acids skeleton.

Introduction

Frankincense is the most precious resin religiously, socially, economically, and medicinally; no other resin was so highly praised and economically valued as frankincense. *Boswellia sacra* is endemic to Oman, and its oleogum resin (frankincense) is known for its superior anti-inflammatory activity [1–3]. This sacred resin contains numerous mono-, sesqui-, di- and triterpenes. Among these, four boswellic acids (BAs), viz. *β*-boswellic acid (BA), 3-*O*-acetyl-β-boswellic acid (ABA), 11-keto-*β*-boswellic acid (KBA) and 3-*O*-acetyl-11-keto-*β*-boswellic acid (AKBA) are the most popular. Both ABA (**1**) and AKBA (**2**) (Fig. 1) have demonstrated exceptional biological activities; hence were selected as precursors for this study [4, 5].

Furthermore, heterocycles containing 1,2,3-triazole scaffolds are known to have a large range of biological activities including antimicrobial [6], anti-HIV [7, 8], antiviral [9], antiallergic [10], and antifungal [11, 12] (Fig. 2).

We were interested to explore the potential and biological activity of the natural products having this scaffold. Previously, several novel analogues of these molecules have been prepared in our laboratory as well as by other groups (Fig. 3) [4, 13–18]. Furthermore, several 1*H*-1,2,3-triazole substituted compounds were synthesized [19] and found to be excellent inhibitors against carbonic anhydrase II (CA II) enzyme [20, 21]. Given the interesting biological activities of both triazole derivatives and boswellic acids, we aimed to synthesize triazole tethered boswellic acids (Fig. 3).

In continuation of our research work on 1*H*-1,2,3-triazole derivatives [19, 22], and on boswellic acids [4, 13–18], we have synthesized novel analogues of ABA (**1**) and AKBA (**2**) (Fig. 2) containing a 1*H*-1,2,3-triazole moiety. The choice of 1*H*-1,2,3-triazole was based on its known activities and its broad range of applications in biochemical, pharmaceuticals, biomedicinal and material sciences [23, 24]. The chemistry

of both boswellic acids and the 1*H*-1,2,3-triazole derivatives have underwent a substitutional growth over the past decades [5, 25].

Carbonic anhydrases (CAs, EC 4.2.1.1) are class of metallo-enzymes using zinc as a cofactor for the reversible inter-conversion of carbon dioxide and bicarbonate [26, 27]. Among the 16 CA isoforms reported so far, only 12 isoforms are catalytically active and varies with respect to their location, kinetic properties, and inhibitor profiles [28, 29]. CAs are involved in different physiological and pathological processes [30–32], as a consequence, they seem to be interesting therapeutic targets to treat pathological disorders [33–35]. CA II is mainly involved in the regulation of the bicarbonate concentration in the eyes. CA II inhibitors can be used to reduce the intraocular pressure usually associated with glaucoma [36–38]. Other than that CA II is also expressed in malignant brain tumors [39], renal, gastritic and pancreatic carcinomas [40–42]. These inhibitors have also been considered as an adjunct in the chemotherapy of cancer. There are number of sulfonamides derivatives reported for CA II inhibitions [43–49].

Herein, we report for the first time the synthesis and *in-vitro* CA II inhibitory activity of a novel series of 1*H*-1,2,3-triazole analogues of ABA and AKBA. Furthermore, some structure-activity relationships, molecular docking, and kinetic studies of the active analogues were discussed.

Results And Discussion

Chemistry

*Synthesis of 1H-1,2,3-triazole analogues of 3-O-acetyl-β-boswellic acid (**10a-d**) and 3-O-acetyl-11-keto-β-boswellic acid (**11a-d**)*

Compounds **1** and **2** were obtained as white crystals from the oleogum resin of *Boswellia sacra* using a modification of Jauch's procedure [50]. In pursuing our aim for synthesizing 1*H*-1,2,3-triazoles, we designed and synthesized a series of novel analogues of ABA and AKBA containing this heterocyclic moiety. The synthesis was performed in four steps (**Scheme 1**).

Thereby, in the initial step, compounds **1** and **2** were treated in DMF with 1-bromo propanol in the presence of potassium carbonate at room temperature to afford the esters **3** (yield 76%) and **4** (yield 74%), respectively [51]. Compound **3** holds a free –OH group, which was converted into tosylated **5** (yield 80%) by its treatment with *p*-toluenesulfonyl chloride in the presence of triethylamine (Et_3N) and 4-dimethylaminopyridine (DMAP) in dry DCM [52]. Under similar conditions, the AKBA derivative **6** was obtained from compound **4** in 83% yield. In the next step, compounds **5** and **6** were treated with sodium azide (NaN_3) in DMF at 70 $^{\circ}$C to afford the corresponding azides **7** and **8** in good yields of 74% and 71%, respectively [53]. The final step was carried out using *"Click"* chemistry. Thereby, a 1,3-dipolar cycloaddition reaction between β-ABA-azide **7** and different alkyne derivatives **9a-d** in the presence of copper iodide (CuI) and Hünig's base in MeCN furnished the desired products, 1*H*-1,2,3-triazole analogues of β-ABA **10a-d** in 68-75% yields [54, 55]. Under similar reaction conditions, the 1*H*-1,2,3-triazole analogues of β-ABA **11a-d** were obtained from azide **8** in 72-76% yields.

In vitro carbonic anhydrase II inhibition

Different 1*H*-1,2,3-triazole derivatives of **1** and **2** were evaluated for their ability to act as inhibitor of CA II. All the assays were carried out at micro molar level using acetazolamide as a standard inhibitor showing an IC_{50} value of 18.2 ± 1.23 μM. After preliminary screening, the parent compounds **1** and **2** held weak activity with IC_{50} values of 55.5 ± 1.32 and 95.5 ± 1.74 μM as compared to the reference compound (Table 1). The addition of bulky groups on different position enhanced their inhibitory activity, and as a result, all compounds (**3**-**11d**) showed significant CA II inhibition with IC_{50} values in the range of 13.2–60.1 μM. Compounds **5** and **10b** were found to be the best inhibitors in this series, while compounds **3**, **7**, **10a**, **10c**, **10d**, **8** and **11c** showed only moderate inhibition with respect to the standard. However, compounds **6** and **11d** were weak inhibitors of this series (Table 1).

Table 1. Carbonic anhydrase II inhibitory potential and molecular docking results of compounds (**3**-**11d**).

Compounds	IC_{50} ± S.E.M* (μM)	Docking Score	Binding Interaction			
			Ligand Atoms	Receptor Atoms	Interactions	Bond Length (Å)
1	55.5 ± 1.32	-5.15	O78	ND2-ASN62	HBA	3.56
			O80	ND2-ASN62	HBA	2.00
			O81	ND2-ASN67	HBA	1.71
2	95.5 ± 1.74	-3.80	O76	NE2-HIS64	HBA	1.55
3	25.4 ± 0.71	-6.54	O77	OG1-THR200	HBA	2.61
			O90	ND2-ASN67	HBA	1.84
			O91	ND2-ASN62	HBA	1.87
4	N.A	---	---	---	---	---
5	13.2 ± 0.51	-10.47	O111	NE2-GLN92	HBA	2.49
			O78	ND2-ASN67	HBA	1.92
			O89	NE2-HIS64	HBA	1.93
			O95	OG1-THR200	HBA	2.88
			6-ring	OG1-THR199	π-H	3.44
			6-ring	ring-TRP209	π-H	2.74
6	60.1 ± 0.65	-5.01	O110	NE2-GLN92	HBA	2.07
			O94	NE2-HIS64	HBA	2.27
7	46.0 ± 0.41	-5.17	N88	N-THR199	HBA	1.77
8	35.4 ± 3. 31	-5.56	N96	N-THR199	HBA	2.54
			O75	ND2-ASN67	HBA	3.14
10a	33.8 ± 1.55	-5.55	N90	N-THR200	HBA	2.97
			O106	NE1-TRP5	HBA	1.81
10b	13.8 ± 0.58	-9.25	N90	N-THR200	HBA	2.09
			O105	ND2-ASN67	HBA	2.75
			O105	ND2-ASN62	HBA	3.45
10c	22.1 ± 1.77	-6.19	O77	ND2-ASN67	HBA	2.47
			O77	ND2-ASN62	HBA	3.13
			N90	OG1-THR200	HBA	3.27
10d	38.9 ± 1.93	-5.50	O95	N-THR199	HBA	2.82
			O78	NE2-GLN92	HBA	3.67
11a	N.A	---	---	---	---	---
11b	N.A	---	---	---	---	---
11c	29.6 ± 1.16	-5.85	O105	ND2-ASN67	HBA	2.43
			N87	NE2-GLN92	HBA	3.09
			N88	NE2-GLN92	HBA	2.96
11d	57.4 ± 2.56	-5.05	N88	N-THR199	HBA	2.52
			O101	NE2-GLN92	HBA	2.24
Acetazolamide*	Standard	18.2 ± 1.23				

*S.E.M = Standard error mean, Acetazolamide = reference compound, N.A = Not Active, HBA = Hydrogen bond acceptor

Kinetics studies

To investigate the mode of interaction and inhibition constant of these potent compounds, some kinetics studies on the most active compounds (**5** and **10b**) were performed applying different concentrations of the test compounds and the substrates. Compounds **5** and **10b** were shown to inhibit CA II in a concentration-dependent manner with *Ki* values of 10.40 ± 0.013 and 14.25 ± 0.017 μM, respectively. From the kinetics studies, it was deduced that **5** and **10b** are non-competitive inhibitors. The type of inhibition was determined from Lineweaver-Burk plots. (Figures 4 and 5).

The K_i values were determined from secondary replots of the Lineweaver-Burk plots by plotting the slope of each line in the Lineweaver-Burk plots against different concentrations of compounds **5** and **10b** (Figure 4B and 5B). The K_i values were confirmed from Dixon plots after plotting the reciprocal of the rate of reaction against different concentrations of compounds **5** and **10b (**Figure 4B and 5B).

Molecular docking and predicted structure-activity relationship

Derivatives of ABA and AKBA (**3, 5-8, 10a-10d, 11c** and **11d**) were targeted at the allosteric site (AS) of human CA II [56]. This revealed that these compounds are fitted neatly at the entrance of the active site between AS1 and AS2. The entrance of the active site of CA II is lined with several hydrophobic residues. The allosteric site 1 (AS1) is located 3-5Å away from the active site and mainly constituted by Val121, Val143, Val207, Trp209, Leu198 and Thr199. AS2 is found near 5-7Å of active site and composed of Tyr7, His64, Asn62, Asn67 and Thr200. Moreover, there is another site present behind the active site where carbon dioxide can bind; this site was termed as AS3 in this study. This site is located 10-12Å far behind the active site and mainly formed by hydrophobic residues like Trp97, Phe226, Val223, Gln222, Val218, Leu157, Leu148, Ala116 and Phe95. All the binding sites are shown in Figure 6.

The most active compound, **5** (IC_{50} = 13.2 ± 0.51µM), demonstrated a 5-fold better activity than the standard 'acetazolamide'. The docked view of **5** revealed that the substituted toluene sulfonic acid fitted deep inside AS1 and held hydrophobic interaction with Trp209, while sulfonic acid interacted with Thr200 of AS2 and Gln92 (lining the active site gorge) through H-bonding. The propyl ester and the acetate group formed H-bonds with the side chain of Asn67 and His64 of AS2, respectively. The triterpene moiety of the compound remained at the entrance of the active site, thus blocking the access to the active gorge. The binding mode of **5** is shown in Figure **7**. Both AS1 and AS2 stabilize the compound at the surface of the enzyme where residues provided strong bonding to the compound and made the compound highest active within this series if compounds. The docking results are tabulated in Table 1.

Among all the compounds, **10b**, **10c**, **3** and **11c** exhibited significant anti-carbonic anhydrase activities, while **10a, 8, 10d** and **7** held moderate inhibitory activities, and **11d** and **6** were the least potent inhibitors. The acetate moiety of **10b** mediated bidentate interactions with the side chains of Asn67 and Asn62,

while the triazole ring interacted with the amino group of Thr200 *via* H-bonding. Additionally, Leu198, Val121 and Val143 provided strong hydrophobic interaction to the triazole substituted trifluoromethyl-phenyl ring of the compound. The triazole nitrogen of **10c** interacted with the -OH of Thr200 through H-bond, while carbonyl oxygen accepted H-bonds from the side chains of Asn67 and Asn62. Similarly, the acetate and carbonyl moieties of compound **3** were stabilized by H-bonding with side chains of Asn62, Asn67 and Thr200. The docked view of **11c** shows that the acetate and the triazolyl groups were linked with the side chains of Asn67 and Gln92 through H-bonding, respectively.

The binding modes of **10a, 8, 10d** and **7** revealed that the acetate and the triazolyl moiety of **10a** formed H-bonds with the side chain and amino group of Trp5 and Thr200, respectively. The amino group of Thr199 mediated H-bonding with the azido group of compounds **7** and **8**, while the propyl acetate group of **8** also interacted with the side chains of Asn67. The acetate group of **10d** accepted a H-bond from the amino group of Thr199 whiles the side chain of Gln92 provided a H-bond to the propyl acetate oxygen of the compound. Compounds **11d** and **6** exhibited least inhibitory potential against CA II *in vitro*. The triazolyl nitrogen of **11d** also accepted a H-bond from the amino group of Thr199 while the acetate group of the compound formed a H-bond with the side chain of Gln92. Likewise, the side chain of Gln92 mediated H-bonding with the sulphate group of **6** which is also H-bonded to the side chain of His64. The docked orientation of **1** showed that both the acetate and the carboxylic groups were stabilized by the side chains of Asn62 and Asn67 *via* H-bonding. However, the carboxylic group of **2** mediated H-bonding with the side chain of His64, while the triterpene group mediated hydrophobic interactions with the sidechains of hydrophobic residues like Phe131, Leu141, Val135, Leu204, and Pro202. We have observed that Asn62, His64, Asn67, Thr200, Thr199, Gln92 played a crucial role in the binding of these compounds at the allosteric site of CA II. The docking scores also correlated with the *in vitro* IC_{50} values. The docked conformations of all the docked compounds are shown in Figure 7, while the bond distances are tabularized in Table 1.

Additionally, we predicted the solubility potential of compounds through logP, logS, and TPSA values. The partition coefficient (logP) of a drug is the ratio of its concentrations in a mixture of two immiscible solvents at equilibrium. In medicinal chemistry, one of the solvents is water (which represent blood serum) and the second is n-octanol which is hydrophobic (indicates lipid bilayer). Hence logP measures hydrophilicity and hydrophobicity of a compound, therefore, estimates the distribution of drugs within the body. Hydrophobic drugs with high octanol-water logP are distributed to hydrophobic areas (lipid bilayers of cells) while hydrophilic drugs (low octanol/water logP) are circulated in aqueous regions (blood serum). Low hydrophilicities and high logP values cause poor absorption or permeation. It has been shown for compounds to have a reasonable propability of being well absorbt their logP value must not be $\geq$ 5.0. The calculated logP of compounds depict that the compounds are highly lipophilic, thus they can easily penetrate the lipid bilayer, however their absorption through the intestine is very low due to their poor solubility or insolubility in the water.

The polar or topological polar surface area (PSA or TPSA) is also a commonly used metric in the medicinal chemistry for the optimization of a compound or a drug's ability to permeate cells. TPSA is

defined as the surface sum over all polar atoms (primarily oxygen and nitrogen with their attached hydrogen atoms) of a compound. Molecules with a PSA of ≥140Å^2 are usually have poor permeability in the cell membranes, however, for molecules which act on CNS, PSA should be ≤90Å^2 in order to effectively penetrate the blood–brain barrier. The TPSA values of compounds **3, 5-8, 10a-10d, 11c** and **11d** were in range of 72.83 to 126.68 Å^2, indicating that these molecules cannot pass blood brain barrier, however, possess moderate permeability to the cell membrane. The results are shown in **Table 2**.

Table 2. The predicted solubility potential of compounds **3, 5-8, 10a-10d, 11c and 11d** in the aqueous and lipid medium.

Compounds	TPSA (Å^2)	logP(o/w)	logS	GIA	BBB Permeant
3	72.83	7.50	-4.514	Low	No
5	95.97	8.98	-4	Low	No
6	113.04	113.04	-4	Low	No
7	77.32	6.74	-4.042	Low	No
8	94.39	5.87	-4.042	Low	No
10a	83.31	8.58	-3.87	Low	No
10b	83.31	9.51	-4.243	Low	No
10c	83.31	8.73	-4.118	Low	No
10d	109.61	6.56	-3.544	Low	No
11c	100.38	7.85	-4.118	Low	No
11d	126.68	5.68	-3.544	Low	No

TPSA= Topological polar surface are, logP(o/w) = Partition coefficient octanol/water, logS = Water solubility, GIA= Gastro-intestinal absorption, BBB Permeant = blood brain barrier permeant

Conclusion

In summary, novel 1*H*-1,2,3-triazole analogues of **1** and **2** were synthesized (**10a-d** and **11a-d**), and evaluated for their CA II inhibitory potential *in vitro*. The C-4 acid group of ABA and AKBA was transformed into an ester containing a hydroxyl group which was modified to an azide through tosylation. The azide compounds were subsequently converted to 1*H*-1,2,3-triazoles having aromatic and ester substituents. Except three compounds (**4**, **11a** and **11b**), all compounds exhibited good inhibitory potential against this enzyme. Kinetic assays demonstrated that these derivatives are non-competitive inhibitors. Additionally, molecular docking indicated that the active compounds have perfectly fitted into the allosteric site of CA II.

Experimental Section

General

Reagents were obtained from Sigma-Aldrich, Germany. Silica gel for column chromatography were of 100-200 mesh. Solvents were purified by following standard procedures. Thin layer chromatography (TLC) was carried using silica gel F_{254} pre-coated plates. UV-light and I_2 stain were used to visualize the spots. The ^{1}H and ^{13}C NMR spectra were recorded on NMR spectrometer (Bruker: 600 MHz for ^{1}H, 150 MHz for ^{13}C and 564 MHz for ^{19}F) using $CDCl_3$ as a solvent. The high-resolution electrospray ionization

mass spectra (HR-ESI-MS) were recorded on Agilent 6530 LC Q-TOF instrument. Organic extracts and solutions of pure compounds were dried over anhydrous $MgSO_4$.

(3-Hydroxypropyl) 3b-acetyloxy-urs-12-en-24-oate (3)

To a solution of **1** (350 mg, 0.702 mmol) in DMF (10 mL), K_2CO_3 (97 mg, 0.702 mmol) and 3-bromo-1-propanol (0.07 mL, 0.773 mmol) were added. After stirring the reaction mixture at room temperature for 18 h, the mixture was diluted with H_2O (45 mL) and extracted with EtOAc (3 × 40 mL). The combined organic layers were washed successively with H_2O (2 × 20 mL), saturated aqueous sodium bicarbonate ($NaHCO_3$), brine (1 × 20 mL), dried over anhydrous magnesium sulfate ($MgSO_4$), filtered, and concentrated in vacuo. The residue was purified by flash column chromatography (silica gel, *n*-hexane/EtOAc, 85:15) to yield **3** (296 mg, 76%) as a white amorphous solid; ^{1}H NMR (600 MHz, chloroform-*d*): δ = 5.30 (d, *J* = 3.4 Hz, 1H), 5.12 (s, 1H), 4.26 (dt, *J* = 12.1, 6.3 Hz, 1H), 4.16 (dt, *J* = 11.7, 6.2 Hz, 1H), 3.70 (t, *J* = 6.2 Hz, 2H), 2.10 (dd, *J* = 12.0, 3.8 Hz, 1H), 2.07 (d, *J* = 5.0 Hz, 3H), 1.98 (dt, *J* = 13.2, 6.8 Hz, 1H), 1.91–1.87 (m, 3H), 1.87–1.66 (m, 6H), 1.66–1.44 (m, 5H), 1.39 (td, *J* = 13.8, 13.0, 6.9 Hz, 4H), 1.33–1.29 (m, 2H), 1.25 (d, *J* = 7.2 Hz, 1H), 1.17 (s, 5H), 1.10 (s, 2H), 1.01 (s, 2H), 0.98 (d, *J* = 6.1 Hz, 2H), 0.90 (d, *J* = 6.0 Hz, 2H), 0.86 (d, *J* = 11.4 Hz, 3H), 0.81 (d, *J* = 6.9 Hz, 3H), 0.78 (d, *J* = 7.2 Hz, 5H) ppm; ^{13}C NMR (150 MHz, chloroform-*d*) δ 176.4, 170.3, 145.0, 139.5, 124.5, 121.7, 73.4, 61.3 , 59.3, 59.1, 50.5, 46.8, 46.7, 42.2, 41.9, 41.5, 40.0, 39.7, 39.6, 37.2, 34.5, 33.8, 33.0, 31.6, 31.2, 28.7, 28.1, 26.5, 23.7, 23.6, 23.3, 23.2, 21.3, 21.3, 19.7, 17.4, 16.8, 13.4 ppm; HRMS (ESI$^+$): Found (M+Na$^+$): 579.4056 $C_{35}H_{56}O_5Na$ required 579.4054.

(3-Hydroxypropyl) 3b-acetyloxy-11-oxo-urs-12-en-24 oate (4)

Following the same procedure as described for the synthesis of **3**, from **2** (350 mg, 0.683 mmol) in DMF (10 mL), K_2CO_3 (94 mg, 0.683 mmol) and 3-bromo-1-propanol (0.07 mL, 0.756 mmol) followed by flash column chromatography (silica gel, *n*-hexane/EtOAc, 85:15) compound **4** (287 mg, 74%) was obtained as a white amorphous solid; ^{1}H NMR (600 MHz, chloroform-*d*): δ = 5.53 (s, 1H), 5.30 (s, 1H), 4.26 (dd, *J* = 11.4, 6.0 Hz, 1H), 4.17 (dd, *J* = 11.4, 5.9 Hz, 1H), 3.70 (t, *J* = 6.1 Hz, 2H), 2.51 (dt, *J* = 13.5, 3.5 Hz, 1H), 2.39 (s, 1H), 2.21–2.15 (m, 1H), 2.07 (s, 4H), 1.89 (q, *J* = 6.3 Hz, 3H), 1.84–1.81 (m, 1H), 1.66 (dd, *J* = 12.9, 3.7 Hz, 1H), 1.61–1.58 (m, 1H), 1.52 (d, *J* = 11.1 Hz, 1H), 1.47 – 1.41 (m, 3H), 1.39–1.36 (m, 2H), 1.33 (s, 3H), 1.30–1.20 (m, 6H), 1.16 (d, *J* = 5.8 Hz, 6H), 1.04 (s, 3H), 0.93 (s, 3H), 0.87 (q, *J* = 6.3, 5.9 Hz, 1H), 0.81–0.77 (m, 6H) ppm; ^{13}C NMR (150 MHz, chloroform-*d*): δ = 199.2, 175.9, 170.2, 164.9, 130.4, 73.2, 61.4, 60.2, 59.2, 59.0, 50.4, 46.7, 45.0, 43.7, 40.9, 39.3, 39.2, 37.2, 34.6, 33.9, 32.8, 31.5, 30.9, 28.8, 27.5, 27.2, 24.0, 23.6, 21.3, 21.1, 20.5, 18.7, 18.3, 17.4, 13.3 ppm; HRMS (ESI$^+$): Found (M+H$^+$): 571.3751 $C_{35}H_{55}O_6$ required 571.3753.

(3-(Tosyloxy)propyl) 3b-acetyloxy-urs-12-en-24-oate (5)

To a solution of compound **3** (270 mg, 0.485 mmol) in dry DCM (25.0 mL), Et_3N (0.14 mL, 0.970 mmol) was added at 0 °C. Then tosyl chloride (102 mg, 0.534 mmol) and a catalytic amount of DMAP (6 mg,

0.0485 mmol) were added. The resulting mixture was allowed to warm to room temperature and stirred for 5 h. The reaction mixture was treated with aqueous 1 N HCl (10 mL), stirred for 10 min and extracted with DCM (3 × 40 mL). The organic layer was washed with saturated $NaHCO_3$ (20 mL) and H_2O (25 mL). The combined organic phases were dried over anhydrous $MgSO_4$ and concentrated under reduced pressure. Flash column chromatography (silica gel, *n*-hexane/EtOAc, 90:10) of the crude product afforded **5** (275 mg, 80%) as a white gummy solid; ^{1}H NMR (600 MHz, chloroform-*d*): δ = 7.77 (d, *J* = 7.9 Hz, 2H), 7.33 (d, *J* = 7.9 Hz, 2H), 5.23 (q, *J* = 2.7 Hz, 1H), 5.17 (d, *J* = 3.8 Hz, 1H), 4.12 (dt, *J* = 12.0, 5.7 Hz, 3H), 4.04 (dt, *J* = 11.7, 6.1 Hz, 1H), 2.43 (s, 3H), 2.06 (d, *J* = 5.0 Hz, 3H), 2.00 (p, *J* = 6.0 Hz, 4H), 1.91–1.83 (m, 2H), 1.67–1.58 (m, 7H), 1.43–1.35 (m, 5H), 1.33–1.26 (m, 4H), 1.23 (s, 3H), 1.09 (s, 5H), 0.98 (s, 3H), 0.94 (s, 1H), 0.90 (d, *J* = 6.0 Hz, 2H), 0.86 (d, *J* = 4.1 Hz, 3H), 0.82 (s, 1H), 0.79–0.76 (m, 4H), 0.72 (d, *J* = 9.4 Hz, 2H) ppm; ^{13}C NMR (150 MHz, chloroform-*d*): δ = 175.7, 170.1, 144.8, 139.5, 132.9, 129.9, 127.8, 124.4, 121.7, 73.3, 66.8, 60.2, 59.1, 50.5, 46.8, 46.7, 42.2, 41.5, 40.0, 39.7, 39.6, 37.2, 34.5, 33.8, 33.0, 31.2, 29.6, 28.7, 28.2, 28.1, 26.5, 23.6, 23.6, 23.5, 23.3, 23.2, 21.6, 21.3, 21.2, 19.7, 17.4, 16.8, 13.3 ppm; HRMS (ESI^+): Found ($M+Na^+$): 733.4103 $C_{42}H_{62}O_7SNa$ required 733.4101.

(3-(Tosyloxy)propyl) 3b-acetyloxy-11-oxo-urs-12-en-24 oate (6)

Following the same procedure as described for the synthesis of compound **5**, from **4** (260 mg, 0.456 mmol) in dry DCM (25.0 mL), Et_3N (0.13 mL, 0.912 mmol), TsCl (95 mg, 0.501 mmol) and cat. amount of DMAP (6 mg, 0.0456 mmol), followed by flash column chromatography (silica gel, *n*-hexane/EtOAc, 90:10) **6** (273 mg, 83%) was obtained as a white amorphous solid; ^{1}H NMR (600 MHz, chloroform-*d*): δ = 7.76 (d, *J* = 8.0 Hz, 2H), 7.34 (d, *J* = 7.9 Hz, 2H), 5.52 (s, 1H), 5.22 (s, 1H), 4.11 (td, *J* = 13.9, 12.8, 5.9 Hz, 3H), 4.07–4.03 (m, 1H), 2.47 (dt, *J* = 13.4, 3.6 Hz, 1H), 2.42 (s, 3H), 2.37 (s, 1H), 2.05 (s, 4H), 1.99 (p, *J* = 6.1 Hz, 3H), 1.89–1.85 (m, 1H), 1.54–1.50 (m, 2H), 1.48–1.41 (m, 3H), 1.39–1.34 (m, 2H), 1.31 (s, 3H), 1.28 (d, *J* = 13.9 Hz, 2H), 1.23 (s, 3H), 1.18 (d, *J* = 4.1 Hz, 1H), 1.13 (s, 3H), 1.09 (s, 3H), 1.00 (dd, *J* = 14.9, 4.1 Hz, 1H), 0.96 (s, 3H), 0.92 (s, 4H), 0.85 (dd, *J* = 10.0, 4.4 Hz, 2H), 0.80 (s, 3H), 0.78 (d, *J* = 6.4 Hz, 2H) ppm; ^{13}C NMR (150 MHz, chloroform-*d*): δ = 199.1, 175.3, 170.0, 164.9, 144.9, 132.8, 130.47, 129.9, 127.8, 73.0, 66.8, 60.4, 60.2, 59.0, 50.3, 46.6, 45.0, 43.7, 40.9, 39.3, 39.2, 37.1, 34.5, 33.9, 32.8, 30.9, 29.6, 28.8, 28.2, 27.5, 27.2, 23.7, 23.5, 21.6, 21.3, 21.1, 20.5, 18.8, 18.3, 17.4, 13.3 ppm; HRMS (ESI^+): Found ($M+H^+$): 725.4007 $C_{42}H_{61}O_8S$ required 725.4009.

(3-Azidopropy) 3b-acetyloxy-urs-12-en-24-oate (7)

A stirred mixture of **5** (260 mg, 0.366 mmol) and NaN_3 (72 mg, 1.098 mmol) in DMF (10 mL) was heated for 3 h at 70 °C, cooled and then treated with ice-water (200 mL). The reaction mixture was extracted with diethyl ether (2 × 150 mL), and the combined extracts were washed successively with water (2×40 mL) and brine (1×30 mL), dried over anhydrous $MgSO_4$, and concentrated in vacuo. The crude product was purified by flash column chromatography (silica gel, *n*-hexane/EtOAc, 92:8) to yield **7** (156 mg, 74%) as a white gummy solid; ^{1}H NMR (600 MHz, chloroform-*d*): δ = 5.29 (q, *J* = 2.5, 2.0 Hz, 1H), 5.15 (dt, *J* = 32.6, 3.7 Hz, 1H), 4.18 (dt, *J* = 12.0, 6.2 Hz, 1H), 4.10 (dt, *J* = 11.6, 6.2 Hz, 1H), 3.41 (t, *J* = 6.7 Hz, 2H), 2.07 (d, *J*

= 5.0 Hz, 4H), 2.00 (dt, *J* = 13.2, 6.5 Hz, 1H), 1.92 (p, *J* = 6.0, 5.3 Hz, 3H), 1.86–1.82 (m, 1H), 1.70 (d, *J* = 4.0 Hz, 2H), 1.67–1.50 (m, 6H), 1.47 (dt, *J* = 13.4, 3.6 Hz, 1H), 1.39 (ddd, *J* = 24.4, 11.1, 4.2 Hz, 4H), 1.31 (d, *J* = 2.9 Hz, 2H), 1.28–1.22 (m, 4H), 1.20 (d, *J* = 4.4 Hz, 1H), 1.17 (s, 3H), 1.10 (s, 2H), 1.04–0.99 (m, 3H), 0.95–0.87 (m, 3H), 0.85 (s, 2H), 0.79 (q, *J* = 8.3, 7.1 Hz, 7H) ppm; ^{13}C NMR (150 MHz, chloroform-*d*) δ 175.9, 170.2, 139.5, 124.4, 121.7, 73.3, 61.3, 59.1, 50.5, 48.3, 46.8, 46.7, 42.2, 41.5, 40.0, 39.7, 39.6, 37.2, 34.5, 33.8, 33.0, 31.2, 28.7, 28.1, 28.0, 26.5, 23.6, 23.3, 23.2, 21.3, 19.7, 17.4, 16.8, 13.3 ppm; HRMS (ESI$^+$): Found (M+Na$^+$): 604.4102 $C_{35}H_{55}N_3O_4Na$ required 604.4105.

(3-Azidopropyl) 3b-acetyloxy-11-oxo-urs-12-en-24-oate (8)

Following the same procedure as described for the synthesis of **7**, from **6** (250 mg, 0.345 mmol) in DMF (10 mL) and NaN_3 (68 mg, 1.035 mmol), followed by flash column chromatography (silica gel, *n*-hexane/EtOAc, 92:8) **8** (145 mg, 71%) was obtained as a white gummy solid; ^{1}H NMR (600 MHz, chloroform-*d*): δ = 5.53 (s, 1H), 5.29 (d, *J* = 2.9 Hz, 1H), 4.19 (dt, *J* = 12.1, 6.2 Hz, 1H), 4.10 (dd, *J* = 11.5, 6.0 Hz, 1H), 3.40 (t, *J* = 6.7 Hz, 2H), 2.51 (dt, *J* = 13.5, 3.5 Hz, 1H), 2.39 (s, 1H), 2.16 (ddd, *J* = 14.1, 11.2, 3.2 Hz, 1H), 2.06 (s, 4H), 1.92 (t, *J* = 6.5 Hz, 2H), 1.86 (dd, *J* = 13.7, 5.2 Hz, 1H), 1.82–1.77 (m, 1H), 1.74 (d, *J* = 3.3 Hz, 1H), 1.66 (s, 3H), 1.60–1.57 (m, 1H), 1.52 (d, *J* = 11.0 Hz, 1H), 1.48–1.42 (m, 3H), 1.39–1.36 (m, 2H), 1.32 (s, 3H), 1.30–1.25 (m, 2H), 1.21 (s, 1H), 1.16 (d, *J* = 2.8 Hz, 6H), 1.03 (s, 3H), 0.92 (s, 3H), 0.87 (t, *J* = 7.3 Hz, 1H), 0.81–0.77 (m, 6H) ppm; ^{13}C NMR (150 MHz, chloroform-*d*): δ = 199.1, 175.4, 170.1, 164.9, 130.4, 73.1, 61.5, 60.2, 59.0, 50.4, 48.3, 46.7, 45.0, 43.7, 40.9, 39.3, 39.2, 37.2, 34.5, 33.9, 32.8, 30.9, 28.8, 27.9, 27.5, 27.2, 23.9, 23.6, 21.3, 21.1, 20.5, 18.8, 18.3, 17.4, 13.3 ppm; HRMS (ESI$^+$): Found (M+H$^+$): 596.3653 $C_{35}H_{54}N_3O_5$ required 596.3651.

General procedure for synthesis of 1H-1,2,3-triazolyl analogues of 3-O-acetyl-β-boswellic acid (10a-d) and 3-acetyl-11-keto-β-boswellic acid (11a-d)

To a solution of **7** (30 mg, 0.052 mmol) or **8** (30 mg, 0.051 mmol) and alkyne **9a-d** (0.062 mmol, 1.2 eq) in acetonitrile (10 mL) were added CuI (20 mg, 0.104 mmol) and Et_3N (0.022 mL, 0.156 mmol) at room temperature, and the mixture was stirred for 3 h. The reaction mixture was diluted with EtOAc (30 mL), 20 mL of aqueous NH_4Cl was added, and the aqueous layer was extracted with EtOAc (3×30 mL), and the combined organic layer was washed with brine (1×20 mL), dried over anhydrous $MgSO_4$, filtered, and the filtrate was concentrated in vacuo. The crude residue was purified by flash column chromatography (silica gel, *n*-hexane/EtOAc, 85:15) to yield **10a-d** (68-75%) or **11a-d** (72-76%), respectively.

(3-(4-Phenyl-1H-1,2,3-triazol-1-yl)propyl) 3b-acetyloxy-urs-12-en-24-oate (10a)

Pale yellow gummy solid; yield = 72%; ^{1}H NMR (600 MHz, chloroform-*d*): δ = 7.81 (d, *J* = 7.6 Hz, 2H), 7.76 (s, 1H), 7.40 (t, *J* = 7.6 Hz, 2H), 7.31 (d, *J* = 7.5 Hz, 1H), 5.32 (d, *J* = 3.9 Hz, 1H), 5.21–5.09 (m, 1H), 4.49 (t, *J* = 6.9 Hz, 2H), 4.17 (dq, *J* = 9.8, 4.9, 3.7 Hz, 1H), 4.13–4.05 (m, 2H), 2.33 (q, *J* = 6.6 Hz, 2H), 2.08 (d, *J* = 5.0 Hz, 4H), 2.02 (s, 1H), 1.98 (dt, *J* = 13.2, 7.1 Hz, 1H), 1.93–1.81 (m, 3H), 1.77–1.72 (m, 2H), 1.62 (d, *J* = 8.9 Hz, 1H), 1.59–1.46 (m, 3H), 1.45–1.38 (m, 4H), 1.31 (s, 2H), 1.24 (q, *J* = 6.4 Hz, 4H), 1.19 (s, 3H), 1.17

(s, 1H), 1.10 (s, 2H), 1.04–1.00 (m, 3H), 0.98 (s, 1H), 0.90 (d, *J* = 6.0 Hz, 2H), 0.85 (s, 3H), 0.81 (s, 3H), 0.79 (d, *J* = 8.4 Hz, 3H) ppm; ^{13}C NMR (150 MHz, chloroform-*d*): δ = 175.8, 170.3, 147.9, 139.5, 130.4, 128.8, 128.2, 125.7, 124.4, 119.7, 73.2, 60.9, 60.3, 59.1, 50.5, 47.2, 46.9, 46.7, 42.2, 41.5, 40.0, 39.7, 39.5, 37.2, 34.5, 33.8, 33.0, 32.5, 31.2, 31.0, 29.4, 28.7, 28.1, 26.5, 23.7, 23.3, 23.2, 21.3, 19.8, 17.4, 16.9, 14.1, 13.4 ppm; HRMS (ESI$^+$): Found (M+H$^+$): 684.4752 $C_{43}H_{62}N_3O_4$ required 684.4754.

(3-(4-(4-(Trifluoromethyl)phenyl)-1H-1,2,3-triazol-1-yl)propyl) 3b-acetyloxy-urs-12-en-24-oate (**10b**)

White gummy solid; yield = 75%; ^{1}H NMR (600 MHz, chloroform-*d*): δ = 7.93 (d, *J* = 8.0 Hz, 2H), 7.86 (s, 1H), 7.67 (d, *J* = 8.0 Hz, 2H), 5.32 (d, *J* = 4.7 Hz, 1H), 5.12 (d, *J* = 3.7 Hz, 1H), 4.51 (q, *J* = 4.9, 2.8 Hz, 2H), 4.19 (dt, *J* = 11.8, 6.0 Hz, 1H), 4.12-4.08 (m, 1H), 2.36–2.33 (m, 2H), 2.08 (d, *J* = 4.6 Hz, 5H), 1.99 (q, *J* = 8.2, 7.8 Hz, 1H), 1.93–1.86 (m, 2H), 1.84–1.78 (m, 1H), 1.65 (d, *J* = 13.8 Hz, 2H), 1.61–1.58 (m, 1H), 1.50–1.47 (m, 1H), 1.41 (dt, *J* = 12.6, 5.8 Hz, 3H), 1.31 (s, 2H), 1.24 (d, *J* = 6.9 Hz, 3H), 1.19 (s, 3H), 1.10 (s, 3H), 1.00 (d, *J* = 24.5 Hz, 6H), 0.90 (d, *J* = 6.0 Hz, 2H), 0.85 (s, 3H), 0.81 (s, 3H), 0.79 (d, *J* = 8.6 Hz, 6H) ppm; ^{13}C NMR (150 MHz, chloroform-*d*): δ = 175.8, 170.2, 146.5, 145.0, 139.5, 133.9, 128.8, 125.8, 125.7, 124.4, 120.5, 73.2, 60.8, 59.1, 50.6, 47.4, 46.9, 46.7, 42.2, 41.5, 40.0, 39.7, 39.6, 37.2, 34.5, 33.8, 33.0, 31.2, 29.4, 28.7, 28.1, 26.5, 23.7, 23.3, 23.2, 21.3, 19.8, 17.4, 16.9, 13.5 ppm; ^{19}F NMR (564 MHz, chloroform-*d*): δ = -62.61ppm; HRMS (ESI$^+$): Found (M+H$^+$): 752.4488 $C_{44}H_{61}F_3N_3O_4$ required 752.4486.

(3-(4-(4-Fluorophenyl)-1H-1,2,3-triazol-1-yl)propyl) 3b-acetyloxy-urs-12-en-24-oate (**10c**)

White amorphous solid; yield = 73%; ^{1}H NMR (600 MHz, chloroform-*d*): δ = .78 (dd, *J* = 8.4, 5.4 Hz, 2H), 7.73 (s, 1H), 7.10 (t, *J* = 8.5 Hz, 2H), 5.32 (d, *J* = 3.8 Hz, 1H), 5.13 (s, 1H), 4.49 (t, *J* = 6.9 Hz, 2H), 4.18 (dt, *J* = 12.0, 6.1 Hz, 1H), 4.09 (dt, *J* = 11.8, 6.1 Hz, 1H), 2.35–2.31 (m, 2H), 2.08 (d, *J* = 4.9 Hz, 4H), 1.99 (q, *J* = 8.1, 7.4 Hz, 1H), 1.93–1.86 (m, 2H), 1.73 (t, *J* = 8.8 Hz, 2H), 1.67–1.60 (m, 5H), 1.54–1.47 (m, 2H), 1.41 (ddd, *J* = 14.0, 10.9, 5.9 Hz, 4H), 1.31 (s, 2H), 1.24 (d, *J* = 5.6 Hz, 5H), 1.19 (s, 4H), 1.10 (s, 2H), 1.02 (s, 3H), 0.90 (d, *J* = 6.0 Hz, 2H), 0.87–0.85 (m, 3H), 0.81 (s, 3H), 0.79 (d, *J* = 6.9 Hz, 3H) ppm; ^{13}C NMR (150 MHz, chloroform-*d*) δ 175.8, 170.2, 163.5, 161.8, 147.0, 139.5, 127.5, 127.4, 124.4, 119.4, 115.8, 115.7, 73.2, 60.8, 59.1, 50.6, 47.2, 46.9, 46.7, 42.2, 41.5, 40.0, 39.7, 39.6, 37.2, 34.5, 33.8, 33.0, 31.2, 29.6, 29.4, 28.7, 28.1, 26.5, 23.6, 23.3, 23.2, 21.3, 21.2, 19.8, 17.4, 16.9, 13.5 ppm; ^{19}F NMR (564 MHz, chloroform-*d*): δ = -113.49 ppm; HRMS (ESI$^+$): Found (M+H$^+$): 702.4751 $C_{43}H_{61}FN_3O_4$ required 702.4753.

Methyl 1-(3-((3b-acetyloxy-urs-12-en-24carbonyl)oxy)propyl)-1H-1,2,3-triazole-4-carboxylate (**10d**)

White gummy solid; yield = 68%; ^{1}H NMR (600 MHz, chloroform-*d*): δ = 8.10 (s, 1H), 5.30 (d, *J* = 3.5 Hz, 1H), 5.15 (dt, *J* = 32.5, 3.7 Hz, 1H), 4.50 (t, *J* = 7.0 Hz, 2H), 4.14 (dt, *J* = 12.1, 6.1 Hz, 1H), 4.08–4.04 (m, 1H), 3.94 (s, 3H), 2.33–2.30 (m, 2H), 2.08 (d, *J* = 5.0 Hz, 4H), 1.99 (dt, *J* = 12.9, 6.3 Hz, 1H), 1.90 (dt, *J* = 10.2, 4.7 Hz, 2H), 1.85–1.81 (m, 1H), 1.66 (s, 2H), 1.75–1.70 (m, 2H), 1.62 (d, *J* = 6.0 Hz, 1H), 1.49 (s, 1H), 1.41 (d, *J* = 10.5 Hz, 2H), 1.38 (s, 1H), 1.31 (s, 2H), 1.24 (d, *J* = 15.2 Hz, 6H), 1.18 (s, 3H), 1.10 (s, 3H), 1.02 (s, 3H), 0.90 (d, *J* = 5.9 Hz, 2H), 0.85 (d, *J* = 4.2 Hz, 3H), 0.80 (s, 3H), 0.78 (d, *J* = 6.1 Hz, 5H) ppm; ^{13}C NMR (150 MHz, chloroform-*d*): δ = 175.8, 170.2, 161.0, 140.1, 139.5, 127.5, 124.4, 73.2, 60.5, 59.1, 52.2, 50.5,

47.6, 46.9, 46.7, 42.2, 41.5, 40.0, 39.7, 39.6, 37.2, 34.5, 33.8, 33.0, 31.2, 29.6, 29.3, 28.7, 28.1, 26.5, 23.6, 23.3, 23.2, 21.3, 21.2, 19.8, 17.4, 16.9, 13.5 ppm; HRMS (ESI^+): Found ($M+H^+$): 666.4444 $C_{39}H_{60}N_3O_6$ required 666.4442.

(3-(4-Phenyl-1H-1,2,3-triazol-1-yl)propyl) 3b-acetyloxy-11-oxo-urs-12-en-24-oate (**11a**)

White amorphous solid; yield = 72%; ^1H NMR (600 MHz, chloroform-*d*): δ = 7.81 (d, *J* = 7.7 Hz, 2H), 7.77 (s, 1H), 7.40 (t, *J* = 7.6 Hz, 2H), 7.32 (d, *J* = 7.5 Hz, 1H), 5.53 (s, 1H), 5.33 (s, 1H), 4.49 (t, *J* = 6.8 Hz, 2H), 4.20 (dt, *J* = 12.1, 6.1 Hz, 1H), 4.09 (dd, *J* = 11.5, 5.7 Hz, 1H), 2.53 (dt, *J* = 13.4, 3.4 Hz, 1H), 2.40 (s, 1H), 2.34 (t, *J* = 6.5 Hz, 2H), 2.21–2.15 (m, 1H), 2.07 (s, 4H), 1.90–1.79 (m, 3H), 1.62 (dd, *J* = 15.4, 3.6 Hz, 2H), 1.52 (d, *J* = 11.1 Hz, 1H), 1.48–1.42 (m, 3H), 1.40–1.37 (m, 2H), 1.32 (s, 3H), 1.29 (s, 1H), 1.23 (d, *J* = 3.1 Hz, 3H), 1.19 (s, 3H), 1.16 (s, 3H), 1.05 (s, 3H), 1.01 (d, *J* = 5.7 Hz, 1H), 0.92 (s, 3H), 0.89–0.85 (m, 1H), 0.81–0.76 (m, 6H) ppm; ^{13}C NMR (150 MHz, chloroform-*d*): δ = 199.1, 175.4, 170.2, 165.0, 130.4, 128.8, 128.2, 125.7, 119.8, 73.0, 61.1, 60.2, 59.0, 50.4, 47.3, 46.7, 45.0, 43.7, 40.8, 39.3, 39.2, 37.2, 34.5, 33.9, 32.7, 30.9, 29.6, 29.4, 28.8, 27.5, 27.2, 23.9, 23.6, 21.3, 21.1, 20.5, 18.8, 18.3, 17.4, 13.4 ppm; HRMS (ESI^+): Found ($M+H^+$): 698.4556 $C_{43}H_{60}N_3O_5$ required 698.4558.

(3-(4-(4-(Trifluoromethyl)phenyl)-1H-1,2,3-triazol-1-yl)propyl) 3b-acetyloxy-11-oxo-urs-12-en-24-oate (**11b**)

White amorphous solid; yield = 76%; ^1H NMR (600 MHz, chloroform-*d*): δ = 7.92 (d, *J* = 8.0 Hz, 2H), 7.87 (s, 1H), 7.65 (d, *J* = 8.1 Hz, 2H), 5.51 (d, *J* = 2.6 Hz, 1H), 5.30 (dt, *J* = 17.7, 2.8 Hz, 1H), 4.50 (td, *J* = 6.9, 4.0 Hz, 2H), 4.19 (dt, *J* = 12.0, 6.1 Hz, 1H), 4.09 (q, *J* = 3.9, 2.9 Hz, 1H), 2.52 (dt, *J* = 13.2, 3.5 Hz, 1H), 2.38 (d, *J* = 6.1 Hz, 1H), 2.35 (q, *J* = 6.6 Hz, 2H), 2.16 (td, *J* = 11.4, 5.9 Hz, 1H), 2.06 (d, *J* = 8.0 Hz, 4H), 1.89–1.75 (m, 6H), 1.68–1.58 (m, 3H), 1.51 (d, *J* = 11.1 Hz, 1H), 1.46–1.36 (m, 6H), 1.31 (s, 3H), 1.17 (s, 3H), 1.14 (s, 3H), 1.03 (s, 3H), 1.00 (d, *J* = 4.7 Hz, 1H), 0.91 (s, 3H), 0.79–0.76 (m, 6H) ppm; ^{13}C NMR (150 MHz, chloroform-*d*): δ = 199.1, 175.4, 170.2, 165.1, 146.5, 133.8, 130.4, 125.8, 120.6, 72.9, 61.0, 60.1, 59.0, 50.4, 47.4, 46.7, 45.0, 43.7, 40.8, 39.3, 39.2, 37.2, 34.5, 33.9, 32.7, 30.8, 29.3, 28.8, 27.4, 27.2, 23.9, 23.7, 21.3, 21.1, 20.5, 18.8, 18.3, 17.4, 14.1, 13.4 ppm; ^{19}F NMR (564 MHz, chloroform-*d*): δ = -62.59 ppm; HRMS (ESI^+): Found ($M+H^+$): 766.0004 $C_{44}H_{59}F_3N_3O_5$ required 766.0002.

(3-(4-(4-Fluorophenyl)-1H-1,2,3-triazol-1-yl)propyl) 3b-acetyloxy-11-oxo-urs-12-en-24-oate (**11c**)

White gummy solid; yield = 74%; ^1H NMR (600 MHz, chloroform-*d*): δ = 7.78 (dd, *J* = 8.5, 5.2 Hz, 2H), 7.74 (s, 1H), 7.10 (t, *J* = 8.3 Hz, 2H), 5.53 (s, 1H), 5.32 (d, *J* = 2.8 Hz, 1H), 4.49 (s, 2H), 4.20 (dt, *J* = 11.4, 5.8 Hz, 1H), 4.10 (q, *J* = 6.2 Hz, 1H), 2.56–2.50 (m, 1H), 2.40 (s, 1H), 2.34 (s, 2H), 2.17 (t, *J* = 14.5 Hz, 1H), 2.07 (s, 5H), 1.87 (dd, *J* = 13.4, 5.2 Hz, 1H), 1.83 (d, *J* = 11.2 Hz, 1H), 1.63 (d, *J* = 3.4 Hz, 2H), 1.52 (d, *J* = 11.1 Hz, 1H), 1.48–1.43 (m, 3H), 1.40–1.37 (m, 2H), 1.32 (s, 3H), 1.29 (s, 1H), 1.23 (d, *J* = 3.1 Hz, 3H), 1.18 (s, 3H), 1.15 (s, 3H), 1.04 (s, 3H), 1.01 (d, *J* = 3.8 Hz, 1H), 0.92 (s, 3H), 0.87 (d, *J* = 8.7 Hz, 1H), 0.80 (s, 3H), 0.78 (d, *J* = 6.5 Hz, 3H) ppm; ^{13}C NMR (150 MHz, chloroform-*d*): δ = 199.0, 175.4, 170.1, 164.9, 163.5, 147.0, 130.4, 127.5, 127.4, 126.6, 119.5, 115.8, 115.7, 72.9, 61.1, 60.2, 59.0, 50.4, 47.3, 46.8, 45.0, 43.7, 40.8, 39.3, 39.2, 37.2, 34.5, 33.9, 32.8, 30.8, 29.3, 28.8, 27.5, 27.2, 23.9, 23.7, 21.3, 20.5, 18.8, 18.3, 17.4, 13.4

ppm; ^{19}F NMR (564 MHz, chloroform-*d*): δ = -113.50 ppm; HRMS (ESI$^+$): Found (M+H$^+$): 716.4799 $C_{43}H_{59}FN_3O_5$ required 716.4801.

Methyl 1-(3-((3b-acetyloxy-11-oxo-urs-12-en-24carbonyl)oxy)propyl)-1H-1,2,3-triazole-4-carboxylate (11d)

White gummy solid; yield = 72%; ^{1}H NMR (600 MHz, chloroform-*d*): δ = 8.10 (s, 1H), 5.53 (s, 1H), 5.30 (d, *J* = 2.8 Hz, 1H), 4.50 (td, *J* = 6.9, 3.8 Hz, 2H), 4.17 (dd, *J* = 11.7, 5.9 Hz, 1H), 4.09–4.04 (m, 1H), 3.94 (s, 3H), 2.53 (dt, *J* = 13.4, 3.5 Hz, 1H), 2.40 (s, 1H), 2.32 (t, *J* = 6.5 Hz, 2H), 2.15 (t, *J* = 14.4 Hz, 1H), 2.08 (s, 4H), 1.89 (dd, *J* = 13.7, 5.1 Hz, 1H), 1.78 (dd, *J* = 24.9, 13.3 Hz, 3H), 1.67 (d, *J* = 17.0 Hz, 2H), 1.54 (s, 1H), 1.49–1.41 (m, 3H), 1.42–1.36 (m, 2H), 1.33 (s, 3H), 1.23 (s, 3H), 1.17 (d, *J* = 10.8 Hz, 6H), 1.04 (s, 3H), 0.93 (s, 3H), 0.87–0.84 (m, 2H), 0.80 (s, 3H), 0.78 (d, *J* = 6.4 Hz, 3H) ppm; ^{13}C NMR (150 MHz, chloroform-*d*): δ = 199.0, 175.4, 170.1, 164.9, 161.0, 130.4, 127.5, 72.9, 60.8, 60.2, 59.0, 52.2. 50.4, 47.6, 46.8, 45.0, 43.7, 40.9, 39.3, 39.2, 37.2, 34.5, 33.9, 32.8, 30.9, 29.6, 29.3, 28.8, 27.5, 27.2, 23.9, 23.6, 21.3, 21.1, 20.5, 18.8, 18.3, 17.4, 13.4 ppm; HRMS (ESI$^+$): Found (M+Na$^+$): 702.3879 $C_{39}H_{57}N_3O_7Na$ required 702.3877.

In-vitro assay for CA II

In this assay, colorless 4-nitrophenyl acetate (4-NPA) is hydrolyzed to yellow 4-nitrophenol[27]. The assay was carried out at 25 ˚C in 20 mM HEPES-Tris buffer of pH 7.4 in 96-well plate. Each well of 96-well plate comprised 140 µL of HEPES-Tris buffer solution, 20 µL of fresh enzyme solution (0.1 mg/mL in buffer) of purified bovine erythrocyte CA II and 20 µL of test compound in DMSO (10% final concentration). The mixture of enzyme and inhibitor was pre-incubated for 15 min at room temperature to allow the formation of the EI complex. After incubation, the reaction was initiated by adding of 20 µL substrate 4-NPA (0.7 mM). For kinetics studies 0.8, 0.4, 0.2 and 0.1 mM of substrate were used. It was followed by continuous measurement of amount of product formed at l = 400 nm for 30 min at 1 min intervals in 96-well flat bottom plates, using ELISA Reader xMARK Microplate spectrophotometer, BIORAD (USA). The activity of control (in the absence of inhibitor) was taken as 100%. The measurements were taken in triplicates at each used concentration [26,28].

The % inhibition was calculated by using the following formula:

% Inhibition = 100-(OD test well/OD control) ×100

Molecular Docking

The X-ray crystallographic structure of CA II in complex with carbon dioxide and bicarbonate ion (PDB code: 2VVB, resolution: 1.66Å) was used in docking. The structures of all the compounds were prepared on ChemDraw software and saved in mol format, then imported into MOE database where each molecule was minimized with MMFF94x force field until an RMSD gradient of 0.1 kcal•mol^{-1}Å^{-1} was achieved, and the partial charges were automatically applied on each molecule during the minimization process. Hydrogen atoms and partial charges were added on the enzyme structure with the default settings of the Protonate 3D protocol in MOE. The binding site was defined by selecting the residues of the allosteric

site. Triangle Matcher placement method and London dG scoring function were used for docking. Later, thirty docked conformations of each compound were saved for conformational sampling. The best docked pose of each compound with respect to the docking score and binding interactions, was selected for SAR analysis.

The logP, logS, and TPSA values of active compounds were calculated by MOE using the 3D-structures of compounds, while gastro-intestinal absorption and blood brain barrier permeability was calculated through SwissADME webserver (http://www.swissadme.ch/index.php).

Declarations

Conflict of interest

All authors confirm that this article content has no conflict of interest.

Acknowledgement

The authors would like to thank the University of Nizwa for the generous support of this project. We thank technical and analytical staff for assistance. The project was funded by The Oman Research Council (TRC) through the funded project (BFP/RGP/CBS/18/011).

References

1. Raffaelli M, Mosti S, Tardelli M (2006) Boswellia sacra Flueck. (Burseraceae) in the Hasik area (Eastern Dhofar, Oman) and a list of the surrounding flora. Webbia 61:245–251
2. Raffaelli M, Mosti S, Tardelli M (2003) The Frankincense Tree (*Boswellia sacra* Flueck., Burseraceae) in Dhofar, southern Oman: field-investigations on the natural populations. Webbia 58:133–149
3. Al-Harrasi A, Ali L, Hussain J, Rehman NU, Mehjabeen, Ahmed M, Al-Rawahi A (2014) Analgesic effects of crude extracts and fractions of Omani frankincense obtained from traditional medicinal plant *Boswellia sacra* on animal models. Asian Pacific J Tropical Med 7:485–490
4. Shamraiz U, Hussain H, Rehman URN, Al-Shidhani S, Saeed A, Khan HY, Khan A, Fischer L, Csuk R, Badshah A, Al-Rawahi A, Hussain J, Al-Harrasi A (2019) Synthesis of new boswellic acid derivatives as potential antiproliferative agents. Nat Pro Res 0:1–8
5. Al-Harrasi A, Hussain H, Csuk R, Khan HY (2018) Chemistry and Bioactivity of Boswellic Acids and Other Terpenoids of the Genus Boswellia. Elsevier, London
6. Genin MJ, Allwine DJ, Anderson DJ, Barbachyn MR, Emmert DE, Garmon SA, Graber DR, Grega KC, Hester JB, Hutchinson DK, Morris J, Reischer RJ, Ford CW, Zurenko GE, Hamel JC, Schaadt RD, Stapert D, Yagi BH (2000) Substituent Effects on the Antibacterial Activity of Nitrogen – Carbon-Linked (Azolylphenyl)oxazolidinones with Expanded Activity Against the Fastidious Gram-Negative Organisms Haemophilus influenzae and Moraxella catarrhalis. J Med Chem 43:953–970

7. Velázquez S, Alvarez R, Pérez C, Gago F, De Clercq E, Balzarini J, Camarasa MJ (1998) Regiospecific synthesis and anti-human immunodeficiency virus activity of novel 5-substituted N-alkylcarbamoyl and N,N-dialkyl carbamoyl 1,2,3-triazole-TSAO analogues. Antiviral Chem Chemotherapy 9:481–489
8. Alvarez R, Velazquez S, San-Felix A, Aquaro S, De Clercq E, Perno CF, Karlsson A, Balzarini J, Camarasa MJ (1994) 1,2,3-Triazole-[2,5-Bis-O-(tert-butyldimethylsilyl)-.beta.-D-ribofuranosyl]-3′-spiro-5″-(4″-amino-1″,2″-oxathiole 2″,2″-dioxide) (TSAO) Analogs: Synthesis and Anti-HIV-1 Activity. J Med Chem 37:4185–4194
9. Pålhagen S, Canger R, Henriksen O, Van Parys JA, Rivière ME. Karolchyk MA (2001) Rufinamide: a double-blind, placebo-controlled proof of principle trial in patients with epilepsy. Epilepsy Res 43:115–124
10. Buckle DR, Rockell CJM, Smith H, Spicer BA (1986) Studies on 1,2,3-triazoles. 13. (Piperazinylalkoxy)-[1]benzopyrano[2,3-d]-1,2,3-triazol-9(1H)-ones with combined H1-antihistamine and mast cell stabilizing properties. J Med Chem 29:2262–2267
11. Fung-Tomc JC, Huczko E, Minassian B, Bonner DP (1998) In Vitro Activity of a New Oral Triazole, BMS-207147 (ER-30346). Antimicrob Agents Chemother 42:313–318
12. Vicentini CB, Brandolini V, Guarneri M, Giori P. Pyrazolo[3,4-d][1,2,3]triazole-1-carboxamides and 5-alkylaminopyrazolo[3,4-d]oxazoles: synthesis and evaluation of the in vitro antifungal activity, Farmaco (Societa Chimica Italiana: 1989). 1992;47:1021–1034
13. Csuk R, Niesen-Barthel A, Barthel A, Kluge R, Ströhl D (2010) Synthesis of an antitumor active endoperoxide from 11-keto-β-boswellic acid. Eur J Med Chem 45:3840–3843
14. Chashoo G, Singh SK, Mondhe DM, Sharma PR, Andotra SS, Shah BA, Taneja SC, Saxena AK (2011) Potentiation of the antitumor effect of 11-keto-β-boswellic acid by its 3-α-hexanoyloxy derivative. Eur J Pharm 668:390–400
15. Csuk R, Barthel-Niesen A, Barthel A, Schäfer R, Al-Harrasi A (2015) 11-Keto-boswellic acid derived amides and monodesmosidic saponins induce apoptosis in breast and cervical cancers cells. Eur J Med Chem 100:98–105
16. Csuk R, Niesen-Barthel A, Schäfer R, Barthel A, Al-Harrasi A (2015) Synthesis and antitumor activity of ring A modified 11-keto-β-boswellic acid derivatives. Eur J Med Chem 92:700–711
17. Li K, Li L, Wang S, Li X, Ma T, Liu D, Jing Y, Zhao L (2017) Design and synthesis of novel 2-substituted 11-keto-boswellic acid heterocyclic derivatives as anti-prostate cancer agents with Pin1 inhibition ability. Eur J Med Chem 126:910–919
18. Saeed A, Hussain H, Shamraiz U, Rehman NU, Khan HY, Badshah A, Heller L, Csuk R, Ali M, Khan A, Al-Harrasi A (2018) Synthesis of new triterpenic monomers and dimers as potential antiproliferative agents and their molecular docking studies. Eur J Med Chem 143:948–957
19. Avula SK, Khan A, Rehman NU, Anwar MU, Al-Abri Z, Wadood A, Riaz M, Csuk R, Al-Harrasi A (2018) Synthesis of 1H-1,2,3-triazole derivatives as new α-glucosidase inhibitors and their molecular docking studies. Bioorganic Chem 81:98–106

20. Kumar R, Vats L, Bua S, Supuran CT, Sharma PK (2018) Design and synthesis of novel benzenesulfonamide containing 1,2,3-triazoles as potent human carbonic anhydrase isoforms I, II, IV and IX inhibitors. Eur J Med Chem 155:545–551
21. Sharma V, Kumar R, Bua S, Supuran CT, Sharma PK (2019) Synthesis of novel benzenesulfonamide bearing 1,2,3-triazole linked hydroxy-trifluoromethylpyrazolines and hydrazones as selective carbonic anhydrase isoforms IX and XII inhibitors. Bioorganic Chem 85:198–208
22. Avula SK, Khan A, Halim SA, Al-Abri Z, Anwar MU, Al-Rawahi A, Csuk R, Al-Harrasi A (2019) Synthesis of novel (R)-4-fluorophenyl-1H-1,2,3-triazoles: A new class of α-glucosidase inhibitors. Bioorganic Chem 91:103182
23. Abdel-Wahab BF, Abdel-Latif E, Mohamed HA, Awad GEA (2012) Design and synthesis of new 4-pyrazolin-3-yl-1,2,3-triazoles and 1,2,3-triazol-4-yl-pyrazolin-1-ylthiazoles as potential antimicrobial agents. Eur J Med Chem 52:263–268
24. Singh N, Pandey SK, Tripathi RP (2010) Regioselective [3 + 2] cycloaddition of chalcones with a sugar azide: easy access to 1-(5-deoxy-d-xylofuranos-5-yl)-4,5-disubstituted-1H-1,2,3-triazoles. Carbohydrate Res 345:1641–1648
25. Thirumurugan P, Matosiuk D, Jozwiak K (2013) Click Chemistry for Drug Development and Diverse Chemical–Biology Applications. Chem Rev 113:4905–4979
26. Arslan O (2001) Inhibition of bovine carbonic anhydrase by new sulfonamide compounds. Biokhimiya 66:1206–1208
27. Pocker Y, Meany JE (1967) The Catalytic Versatility of Erythrocyte Carbonic Anhydrase. II. Kinetic Studies of the Enzyme-Catalyzed Hydration of Pyridine Aldehydes. Biochemistry 6:239–246
28. Shank RP, Doose DR, Streeter AJ, Bialer M (2005) Plasma and whole blood pharmacokinetics of topiramate: the role of carbonic anhydrase. Epilepsy Res 63:103–112
29. Shaik NA, Bokhari HA, Masoodi TA, Shetty PJ, Ajabnoor GMA, Elango R, Banaganapalli B. Molecular modelling and dynamics of CA2 missense mutations causative to carbonic anhydrase 2 deficiency syndrome, Journal of Biomolecular Structure and Dynamics. 2019;1–14
30. Ozensoy Guler O, Capasso C, Supuran CT (2016) A magnificent enzyme superfamily: carbonic anhydrases, their purification and characterization. J Enz Inhib Med Chem 31:689–694
31. Lindskog S (1997) Structure and mechanism of carbonic anhydrase. Pharmacol Ther 74:1–20
32. Aggarwal M, Boone CD, Kondeti B, McKenna R (2013) Structural annotation of human carbonic anhydrases. J Enz Inhib Med Chem 28:267–277
33. Krishnamurthy VM, Kaufman GK, Urbach AR, Gitlin I, Gudiksen KL, Weibel DB, Whitesides GM (2008) Carbonic Anhydrase as a Model for Biophysical and Physical-Organic Studies of Proteins and Protein – Ligand Binding. Chem Rev 108:946–1051
34. Supuran CT (2008) Carbonic anhydrases: novel therapeutic applications for inhibitors and activators. Nat Rev Drug Dis 7:168–181

35. Chegwidden WR, Dodgson SJ, Spencer IM. The roles of carbonic anhydrase in metabolism, cell growth and cancer in animals. Exs. 2000:343–363
36. Ruusuvuori E, Kaila K (2014) Carbonic anhydrases and brain pH in the control of neuronal excitability. Sub-Cellular Biochemistry 75:271–290
37. Pastorekova S, Parkkila S, Pastorek J, Supuran CT (2004) Carbonic anhydrases: Current state of the art, therapeutic applications and future prospects. J Enz Inhib Med Chem 19:199–229
38. Supuran CT, Scozzafava A (2007) Carbonic anhydrases as targets for medicinal chemistry. Bioorganic Med Chem 15:4336–4350
39. Parkkila AK, Herva R, Parkkila S, Rajaniemi H (1995) Immunohistochemical demonstration of human carbonic anhydrase isoenzyme II in brain tumours. Histo Chem J 27:974–982
40. Pastorekova S, Parkkila S, Parkkila AK, Opavsky R, Zelnik V, Saarnio J, Pastorek J (1997) Carbonic anhydrase IX, MN/CA IX: Analysis of stomach complementary DNA sequence and expression in human and rat alimentary tracts. Gastroenterology 112:398–408
41. Frazier ML, Lilly BJ, Wu EF, Ota T, Hewett-Emmett D (1990) Carbonic anhydrase II gene expression in cell lines from human pancreatic adenocarcinoma. Pancreas 5:507–514
42. Parkkila S, Rajaniemi H, Parkkila AK, Kivelä J, Waheed A, Pastoreková S, Pastorek J, Sly WS. Carbonic anhydrase inhibitor suppresses invasion of renal cancer cells. Proceedings of the National Academy of Sciences. 2000;97:2220–2224
43. Yang C, Wang J, Cheng Y, Yang X, Feng Y, Zhuang X, Li Z, Zhao W, Zhang J, Sun X, He X (2020) N-Quinary heterocycle-4-sulphamoylbenzamides exert anti-hypoxic effects as dual inhibitors of carbonic anhydrases I/II. Bioorganic Chem 100:103931
44. Moi D, Nocentini A, Deplano A, Osman SM, AlOthman ZA, Piras V, Balboni G, Supuran CT, Onnis V (2020) Appliance of the piperidinyl-hydrazidoureido linker to benzenesulfonamide compounds: Synthesis, in vitro and in silico evaluation of potent carbonic anhydrase II, IX and XII inhibitors. Bioorganic Chem 98:103728
45. Ghorai S, Pulya S, Ghosh K, Panda P, Ghosh B, Gayen S (2020) Structure-activity relationship of human carbonic anhydrase-II inhibitors: Detailed insight for future development as anti-glaucoma agents. Bioorganic Chem 95:103557
46. George RF, Said MF, Bua S, Supuran CT (2020) Synthesis and selective inhibitory effects of some 2-oxindole benzenesulfonamide conjugates on human carbonic anhydrase isoforms CA I, CA II, CA IX and CAXII. Bioorganic Chem 95:103514
47. Chiaramonte N, Bua S, Angeli A, Ferraroni M, Picchioni I, Bartolucci G, Braconi L, Dei S, Teodori E, Supuran CT, Romanelli MN (2019) Sulfonamides incorporating piperazine bioisosteres as potent human carbonic anhydrase I, II, IV and IX inhibitors. Bioorganic Chem 91:103130
48. Tanini D, Capperucci A, Scopelliti M, Milaneschi A, Angeli A, Supuran CT (2019) Syntesis of thio- and seleno-acetamides bearing benzenesulfonamide as potent inhibitors of human carbonic anhydrase II and XII. Bioorganic Chem 89:102984

49. Lolak N, Akocak S, Bua S, Koca M, Supuran CT (2018) Design and synthesis of novel 1,3-diaryltriazene-substituted sulfonamides as potent and selective carbonic anhydrase II inhibitors. Bioorganic Chem 77:542–547
50. Jauch J, Bergmann J. An Efficient Method for the Large-Scale Preparation of 3-O-Acetyl-11-oxo-β-boswellic Acid and Other Boswellic Acids, Eur J Org Chem. 2003;4752–4756
51. Cheng KG, Su CH, Yang LD, Liu J, Chen ZF (2015) Synthesis of oleanolic acid dimers linked at C-28 and evaluation of anti-tumor activity. Eur J Med Chem 89:480–489
52. Yadav JS, Thrimurtulu N, Uma Gayathri K, Subba Reddy BV, Prasad AR (2008) The stereoselective total synthesis of xestodecalactone C and epi-sporostatin via the Prins cyclisation. Tetrahedron Lett 49:6617–6620
53. Baran PS, Zografos AL, O'Malley DP (2004) Short Total Synthesis of (±)-Sceptrin. J A Chem Soc 126:3726–3727
54. Huisgen R (1963) 1,3-Dipolar Cycloadditions. Past and Future. Angew Chem Int Ed 2:565–598
55. Bera S, Linhardt RJ (2011) Design and Synthesis of Unnatural Heparosan and Chondroitin Building Blocks. J Org Chem 76:3181–3193
56. Domsic JF, Avvaru BS, Chae UK, Gruner SM, Agbandje-McKenna M, Silverman DN, McKenna R (2008) Entrapment of carbon dioxide in the active site of carbonic anhydrase II. J Bio Chem 283:30766–30771

Figures

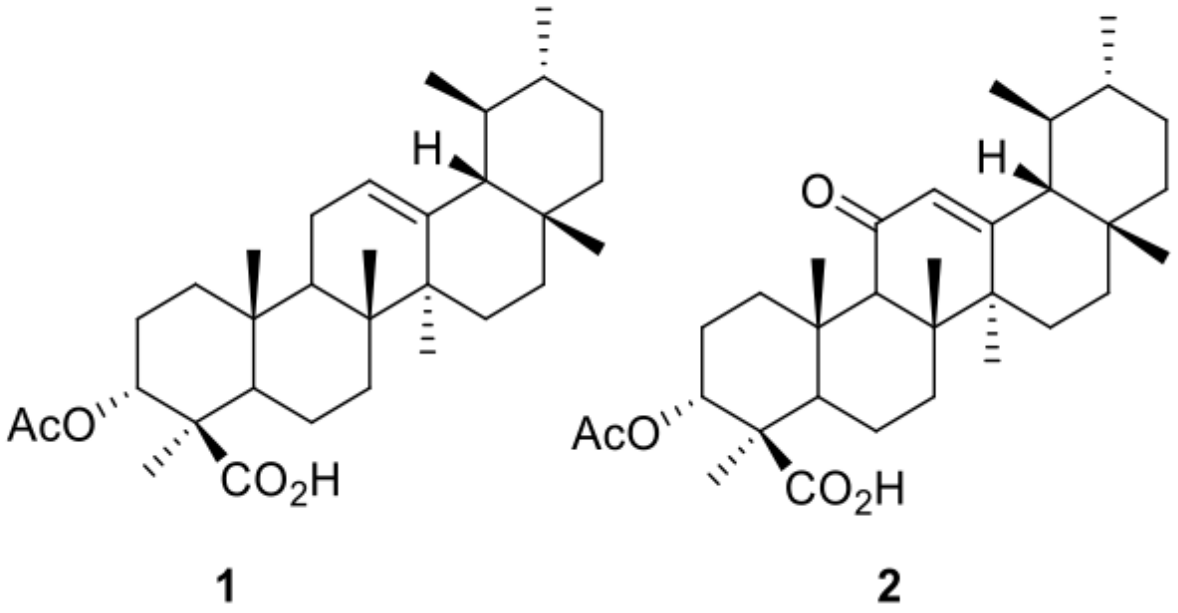

Figure 1

Structures of ABA (1) and AKBA (2)

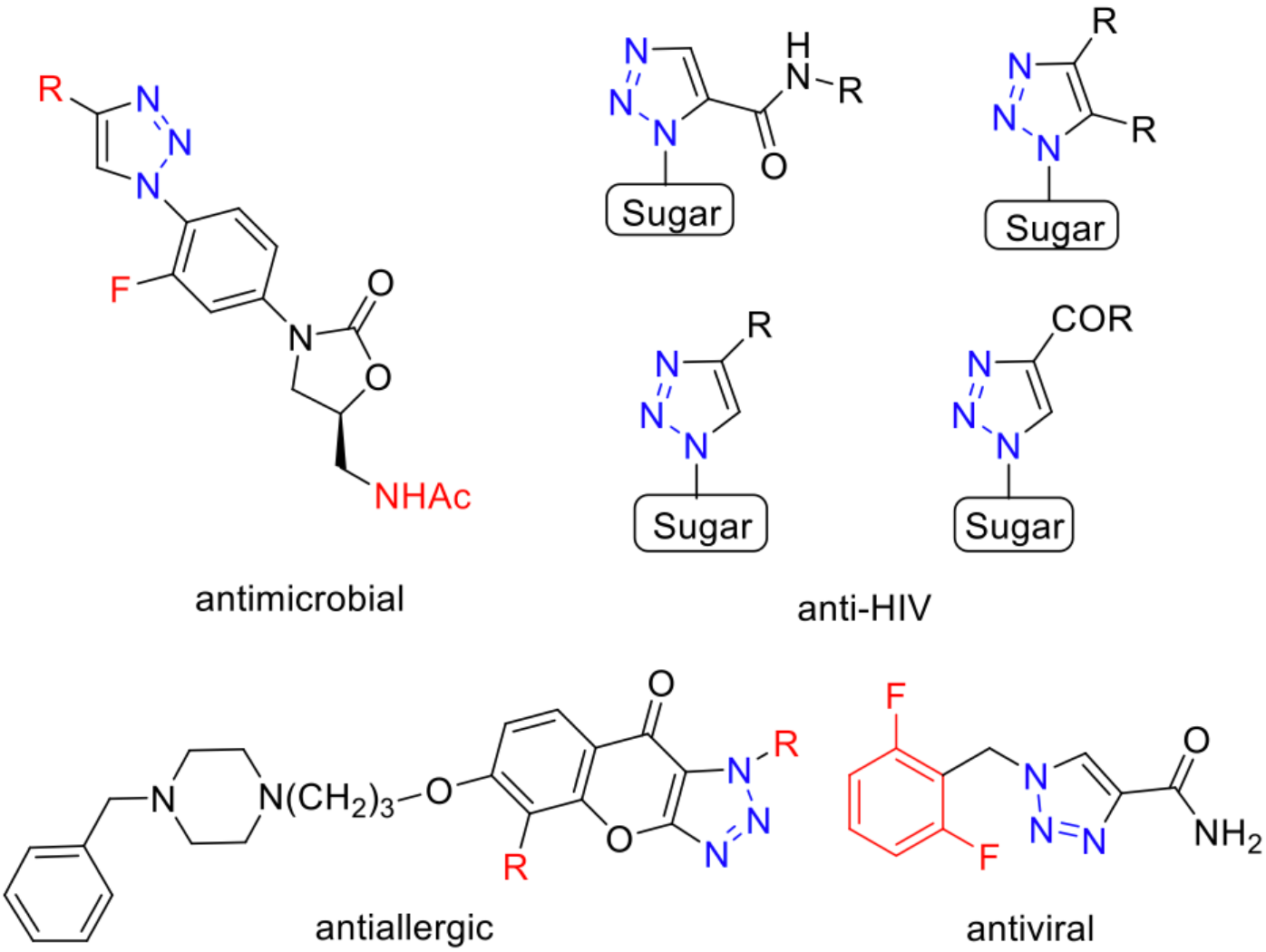

Figure 2

Chemical structures of some clinically used 1H-1,2,3-triazole derivatives.

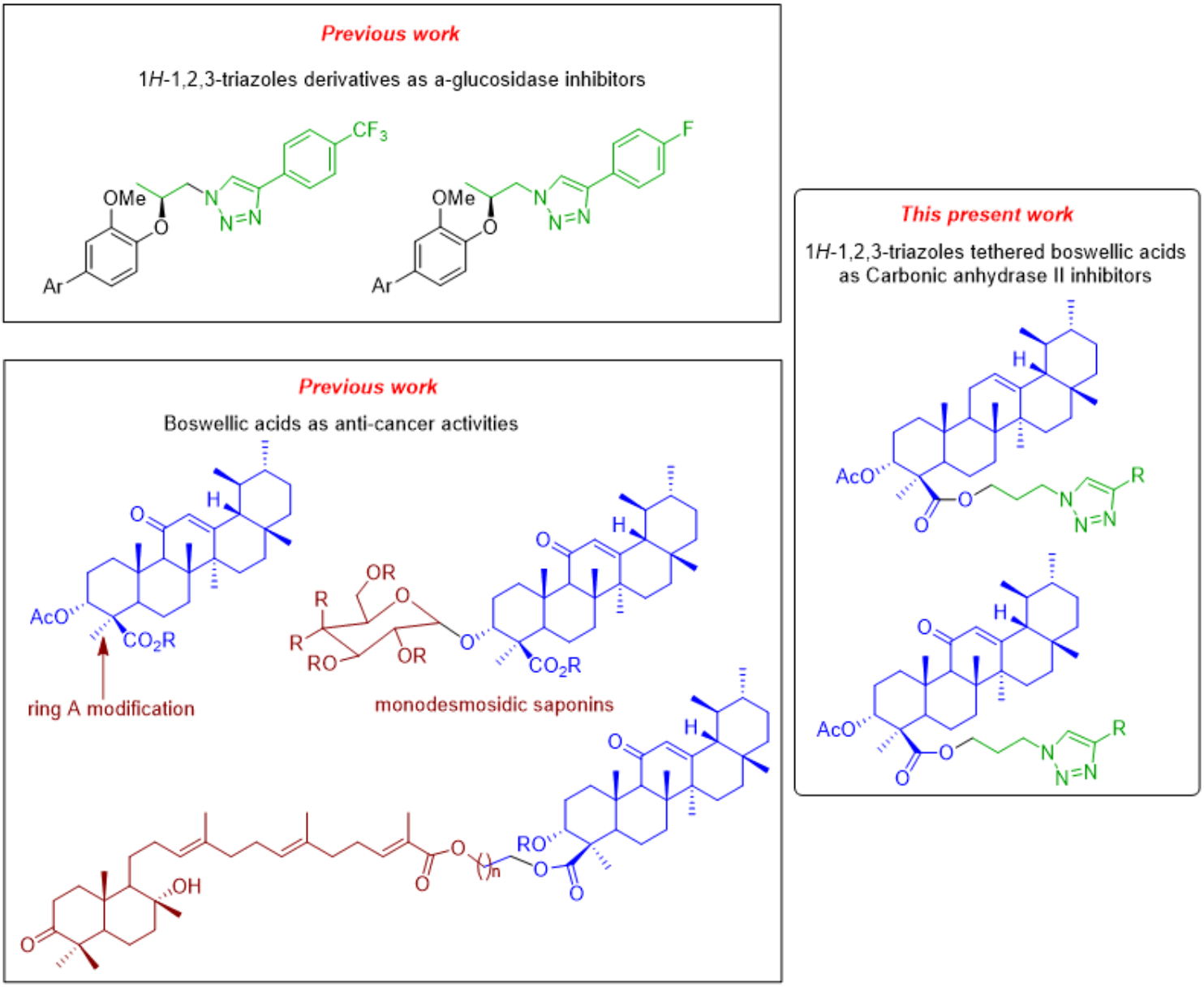

Figure 3

Selective previous work on 1H-1,2,3-triazole analogues, boswellic acids and current work on triazole tethered boswellic acids.

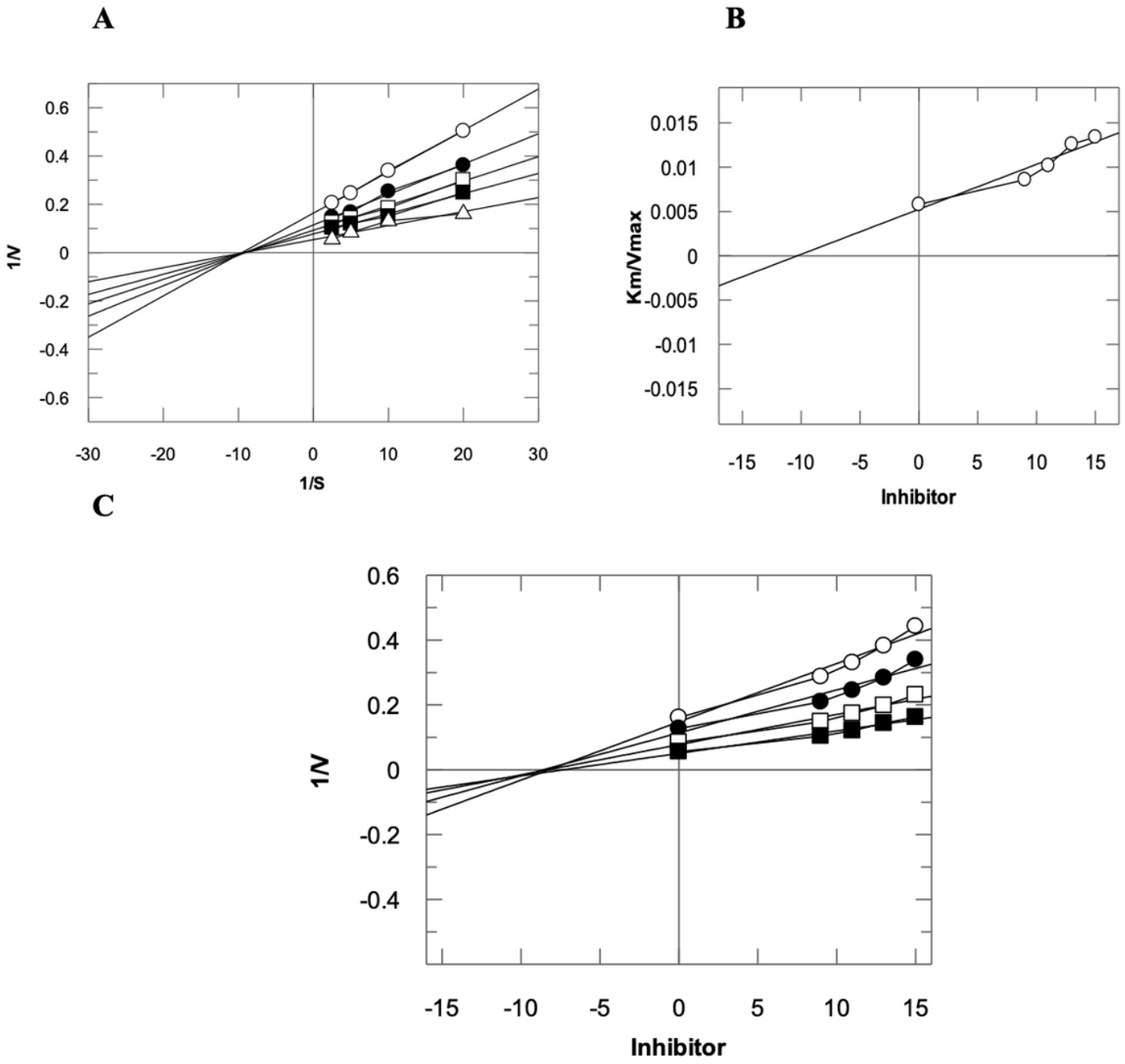

Figure 4

Carbonic anhydrase-II inhibition by compound 5, (A) Lineweaver-Burk plot of reciprocal rate of reaction1/v against reciprocal of substrate 1/s (P-nitrophenyl acetate) in the absence (Δ) and in the presence of 6 μM (■), 9μM (□), 12 μM (●) 15 μM (●) of compound 5. (B) Secondary replot of Lineweaver-Burk plot is between slopes of each line on the Line-weaver Burk vs different concentrations of compound 5, and (C) Dixon plot reciprocal of rate of reaction vs different concentrations of compound 5.

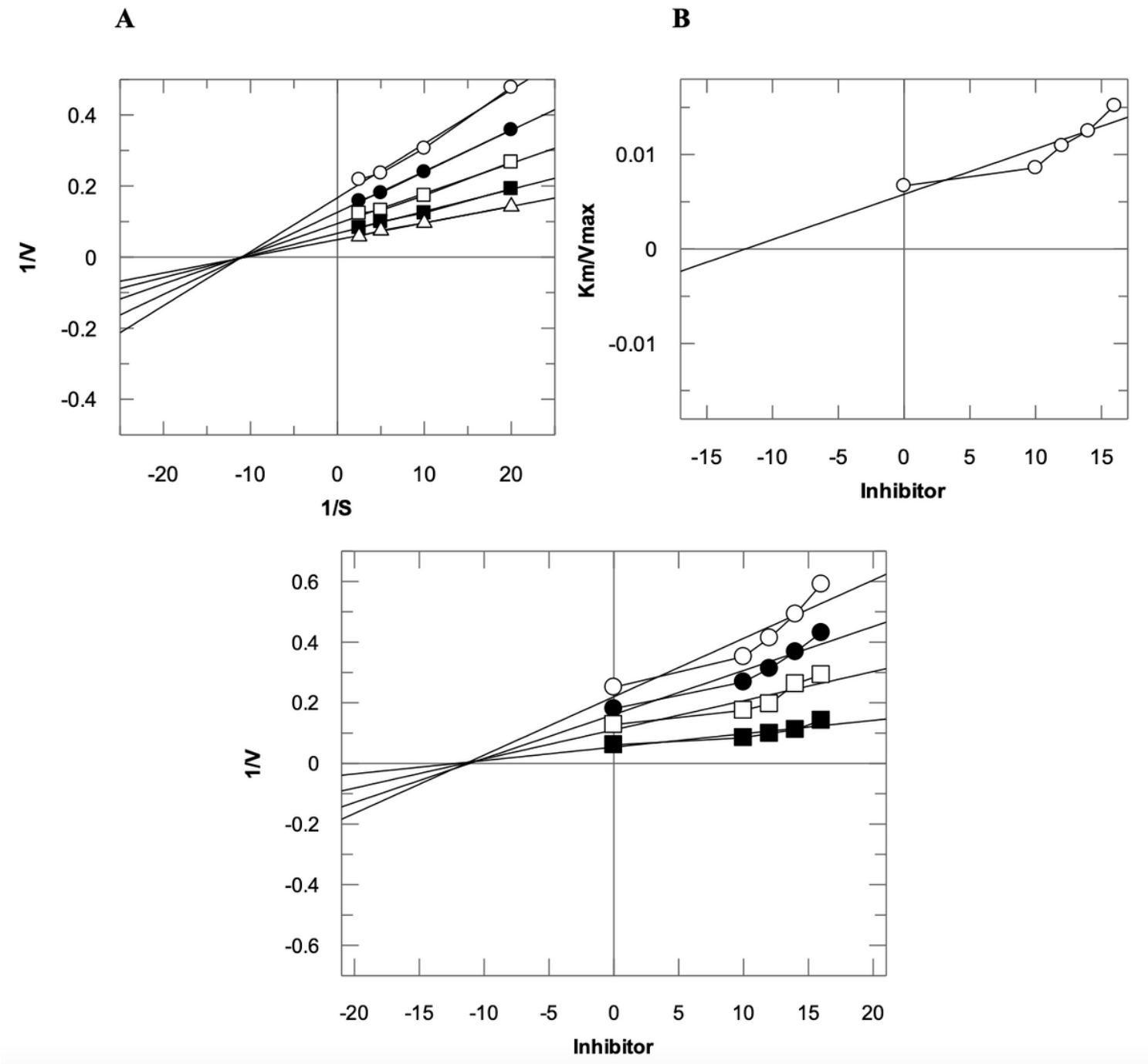

Figure 5

Carbonic anhydrase-II inhibition by compound 10b, (A) Lineweaver-Burk plot of reciprocal rate of reaction1/v against reciprocal of substrate 1/s (P-nitrophenyl acetate) in the absence (Δ) and in the presence of 16 μM (■), 13 μM (□), 10 μM (●) 7 μM (●) of compound 10b. (B) Secondary replot of Line-weaver Burk plot is between slopes of each line on Line-weaver Burk vs different concentrations of compound 10b, and (C) Dixon plot reciprocal of rate of reaction vs different concentrations of compound 10b.

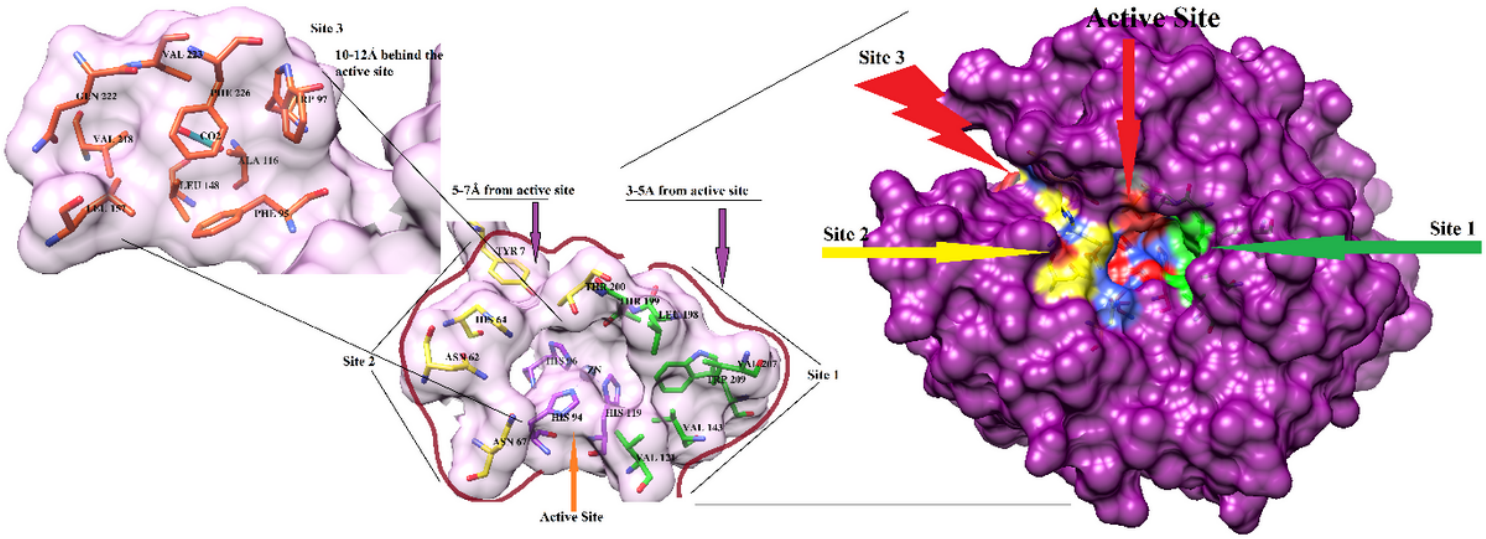

Figure 6

3D-structure of human CA II is illustrated in purple in a surface model. The active site, allosteric sites (AS) 1, 2 and 3 are shown in red, green, yellow and coral surface, respectively. The active site residues are presented in purple sticks, while the residues of AS1, AS2 and AS3 are shown in green, yellow and coral stick models, respectively.

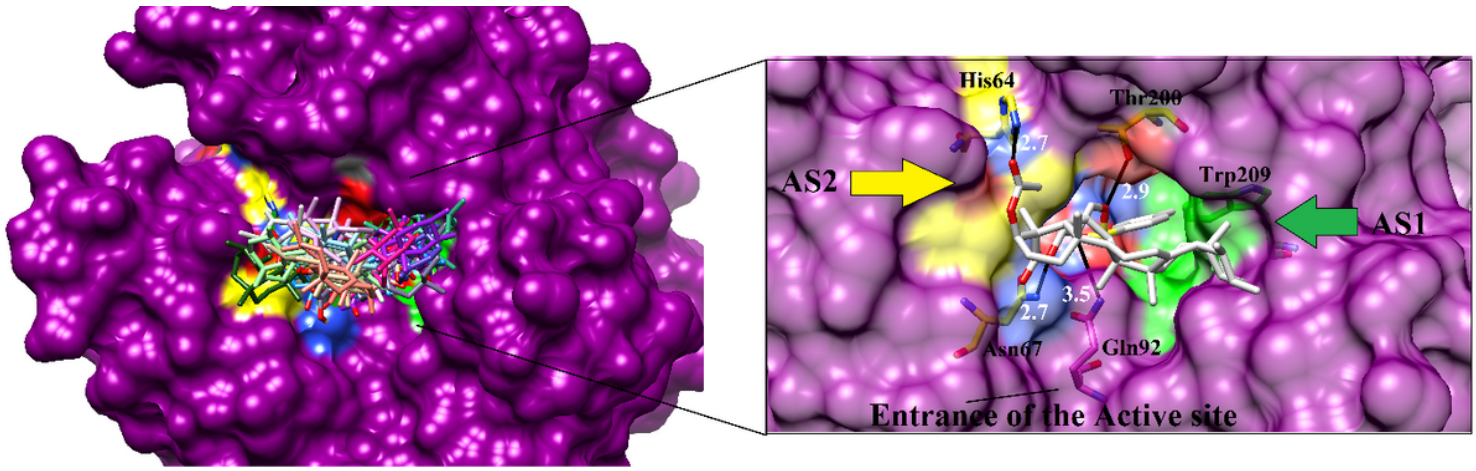

Figure 7

(A) The docked conformations of compounds 3, 5-8, 10a-10d, 11c and 11d are presented at the allosteric site of human CA II. The binding mode of most active compound 5 is highlighted in box at the non-competitive site of CA II. The binding residues of AS1 and AS2 are shown in green and yellow sticks, respectively, ligand is presented in light grey stick model, H-bonds are shown in black lines and the bond length is labelled in white color.

Supplementary Files

This is a list of supplementary files associated with this preprint. Click to download.

- GraphicalAbstract.jpg
- Onlinefloatimage4.png